Computational and Theoretical Chemistry 1035 (2014) 1–5

Contents lists available at ScienceDirect

Computational and Theoretical Chemistry

journal homepage: www.elsevier.com/locate/comptc

Iron complexes of nanodiamond: Theoretical approach

Naveicy Mar, L. Enrique Sansores, Estrella Ramos, Roberto Salcedo *

Instituto de Investigaciones en Materiales, Universidad Nacional Autónoma de México, Circuito Exterior s/n, Ciudad Universitaria, Coyoacán 04510, Mexico City, Mexico

ARTICLE INFO

Article history:
Received 13 December 2013
Received in revised form 17 February 2014
Accepted 17 February 2014
Available online 25 February 2014

Keywords:
Nanodiamond metallic complexes
Theoretical study
Semiconductor behavior

ABSTRACT

Simulated compounds have been proposed for organometallic clusters of nanodiamond with iron; the complexes take advantage of carboxylic ending in order to form a comprehensive bond with the metal ion. The performance is notorious; it seems that the control of electronic behavior is localized on both, the metallic atom and the carboxylic fragments, but not on the intrinsic nanodiamond unities, however, the presence of these nanodiamond ligands is fundamental to establish a sort of electronic confinement, which is responsible of the peculiar electronic behavior. The nature of the frontier molecular orbitals is also studied.

1. Introduction

Nanodiamond is a material that has been the object of several studies over the last few years [1]. This material has varying properties depending on purity, size, phase, etc. [2]. Diamond nanoparticles have drawn significant attention from a wide range of researchers for use in a variety of applications including plating; lubricating oils; polishing and biomedical devices [3]. The production of large quantities of sub 10 nm nanodiamonds involves a top-down approach, which includes milling luminescent high pressure, high temperature (HPHT) microdiamonds into 7 nm particles and then forming water dispersible colloidal quasi-spherical nanodiamonds [4].

There are several features to consider concerning the morphology of a nanodiamond. The size of the clusters is important for stability reasons. Galli and Barnard [5] have suggested that a large nanodiamond cluster consists of three parts, first a diamond core made up of sp^3 hybridized carbon atoms, a superior fullerene-like shell of sp^2 carbon atoms and a surface where all the dangling bonds are completed with either hydrogen or functional groups. Therefore, it is predictable that a nanodiamond particle would be different from others at the surface with different properties, although the core may be similar in all cases. The main method for synthesis of this material involves detonation [6]; this feature implies that the parent substance used as explosive will be responsible for the dopants that may form part of the clusters and therefore it is possible to have several different kinds of material depending on their origin.

The size of nanodiamond nanoparticles can vary from 1.7 to 5.2 nm [7]. Thus the smallest particle is the size of three fullerene (C_{60}) spheres, and it is predictable that any of these could manifest point group symmetry. Due to this feature, it is difficult to design a model for general study. Likewise, it has been observed that many nanoparticles have a metal [8], boron, silicon or nitrogen dopant [9]; and any of these will change dramatically their properties. Again, it is possible to discover different materials proffering a variety of applications. All these ideas suggest that it is possible to design smaller molecules, which manifest nanodiamond properties.

The main goal of this work is to propose an iron organometallic complex, which manifest nanodiamond properties. The design of the molecules in this study is in agreement with the restrictions and characteristics of large nanodiamond particles and take advantage of these, as well as it corresponds to the intrinsic chemistry of metallic clusters. They represent a semiconductor species.

2. Methods

Calculations were carried out using a pure DFT method for energy evaluations, applying Becke's gradient corrections [10] for exchange and Perdew–Wang's for correlation [11]. This is the scheme for the BPW91 method that forms part of the Gaussian 09 Package [12]. All calculations were performed using the 6-31G** basis set. Frequency calculations were carried out at the same level of theory in order to confirm that the optimized structures were at a minimum of the potential surfaces. To estimate the magnetic moment NMR calculations were performed with the GIAO method [13].

3. Results and discussion

In order to evaluate the effect on the electronic properties due to the size and the shape of the cluster, different fragments of

* Corresponding author.
E-mail address: salcedo@unam.mx (R. Salcedo).

http://dx.doi.org/10.1016/j.comptc.2014.02.017
2210-271X/

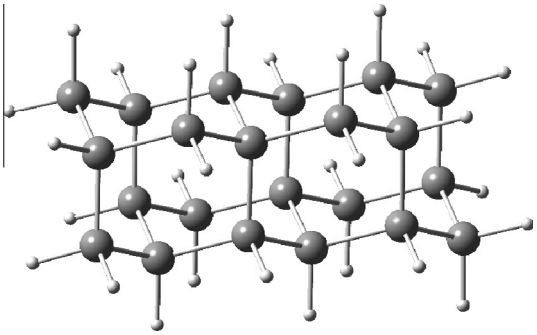

Fig. 1. Structure of a nanodiamond cluster ($C_{22}H_{28}$).

nanodiamonds were optimized as the first task. An sp^3 set of 12, 22, 29 and 35 carbon atoms saturated by hydrogen atoms was chosen (C_xH_y, x = 12, 22, 29, 35; y = 22, 28, 36, 36). The analysis is centered in the cluster of 22 carbon atoms. Therefore, the results for the x = 12, 29, 35 systems are mentioned when they are necessary.

The shape of the nanodiamond ligand with x = 22 can be seen in Fig. 1.

The fragment was chosen as to represent a pristine sp^3 center that belongs to the C_{2h} point group and is therefore expected to manifest all the characteristics of a pure nanodiamond (i.e. electrical insulator, low reactivity, high net energy, etc.), likewise this sample has no secondary structures. Other authors [14] have suggested units of this kind, but in this case, the sample was constructed searching for the preservation of symmetry in the new clusters.

The strategy consists in comparing the molecular orbital schemes of all the analyzed structures. Several features have been taken into account. In first place, the intrinsic size of the nanodiamond ligands, in second instance, the presence or absence of external ligands on the clusters, and in the final item the adopted arrangement of the carboxylic ligands around the iron atom.

The molecules under study were designed following a same model, i.e. a central iron atom joint to two nanodiamond ligands bearing carboxylic ligands as chelating agents. The result should be a square planar coordination complex, however there are important distortions in all cases. They will be described in each particular case. It is obvious that the iron complexes with six coordination are more stable, besides the tetrahedral four coordination are also common for a first row metal, however in the present case the geometry was adopted because the optimization of the geometry in the four coordination case yield these results. A forthcoming work is prepared in which the six coordination case will be shown.

Firstly, the reason to choose nanodiamond clusters as ligands was the insulator nature of these species. The insulator behavior is shown in the corresponding diagram portraying molecular

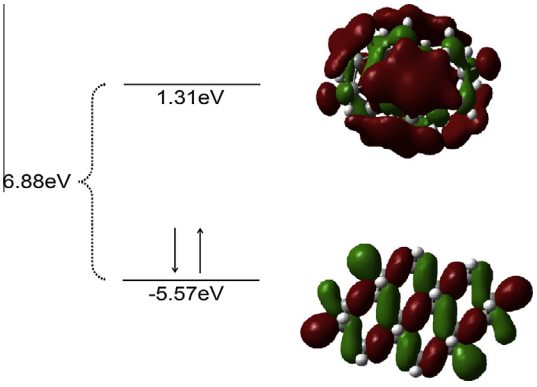

Fig. 2. Frontier molecular orbitals diagram of a nanodiamond ($C_{22}H_{28}$).

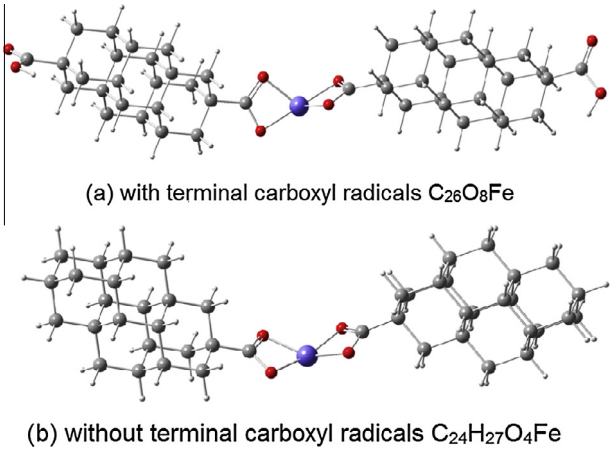

Fig. 3. Iron coordination complexes of nanodiamond $C_{22}H_{28}$.

orbital interaction in Fig. 2. It is possible to see that the energy difference between HOMO and LUMO is 6.88 eV and indeed the LUMO shows a positive value making it difficult for this species to react.

The second step was to build the complexes. For this task, two carboxyl radicals substituted at the edges of the molecule were chosen. There are two potential designs for this sample; the first one has the inner carboxyl radicals interacting with the metal atom, in addition to two more at the extreme edges that can work as trappers of other metals or reactive points. The second one is the same shape for the inner radical and the iron atom, but without terminal trappers. These structures are presented in Fig. 3.

The effect of the size of the nanodiamond units was studied changing the ligands on the two models showed above.

The first notorious feature appears at this point, the structures shown in Fig. 3 present a center with a puckered square. Most iron complexes have a tendency to belong to the *T* or *Td* point group. There are only a few complexes that belong to the D_{4h} point group; all of them may present certain distortions, which arise from steric effects, dangling bonds, etc. In the present case, the center shows a puckered D_{2d} structure, depicting geometry not commonly found in this kind of molecule. It seems that there is not enough strong steric impediment around the aforementioned center. Therefore, it is probable that this distortion arises only from electronic reasons. The electronic behavior of both derivatives is very interesting, but in fact very different in each case, thus they deserve to be analyzed individually.

The first case is the molecule with terminal carboxyl radicals ($C_{26}O_8Fe$). The behavior is practically that of a strong semiconductor species. The molecular orbitals diagram is presented in Fig. 4.

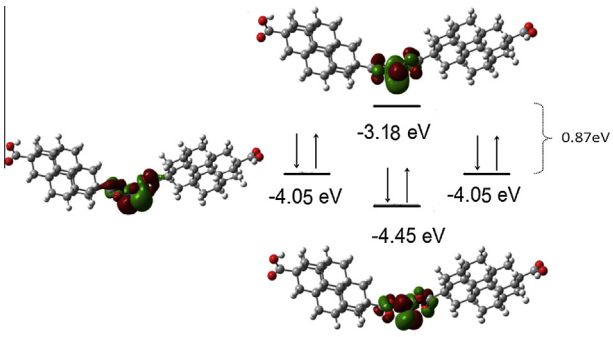

Fig. 4. Frontier molecular orbital diagram of compound ($C_{26}O_8Fe$).

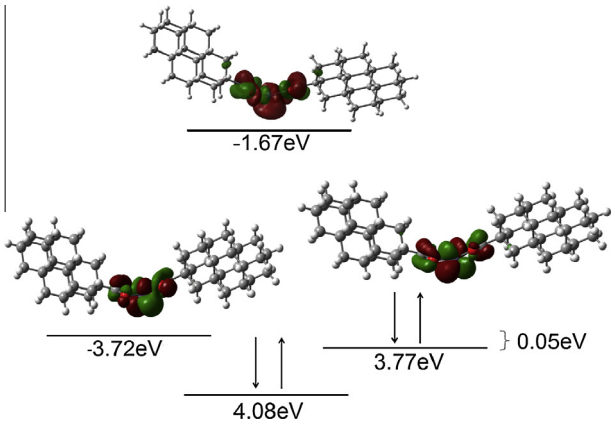

Fig. 5. Molecular orbital diagram of ($C_{24}H_{27}O_4Fe$).

An important effect arises at this point. The presence of new substituents on the ligands causes a decrease on the pseudo-symmetry of the fragment and later another decrement caused by the coordination with the iron atom. Therefore there are no possibilities for a degenerated set of orbitals. However, the HOMO of the species is a two-folded degenerated set. This is a classic example of an accidental degeneracy that is preserved even when the symmetry is reduced. This feature makes way for the possibility of an interaction between four electrons with the upper virtual orbitals (i.e. strong electronic flow) furthermore, the HOMO and the LUMO are very near, and indeed the energy gap between HOMO and LUMO is only 0.87 eV. All the eigenfunctions are centered on the set formed by the iron atom and both inner carboxylic groups. Therefore, this substance must manifest strong semiconductor behavior in spite of the insulating nature of the sole ligand.

The other case ($C_{24}O_4Fe$) without the terminal radicals is much more interesting. The energy gap is large, taking into account the HOMO and the LUMO+1, 2.09 eV, which can be considered as an acceptable value for a semiconductor species. However, where is

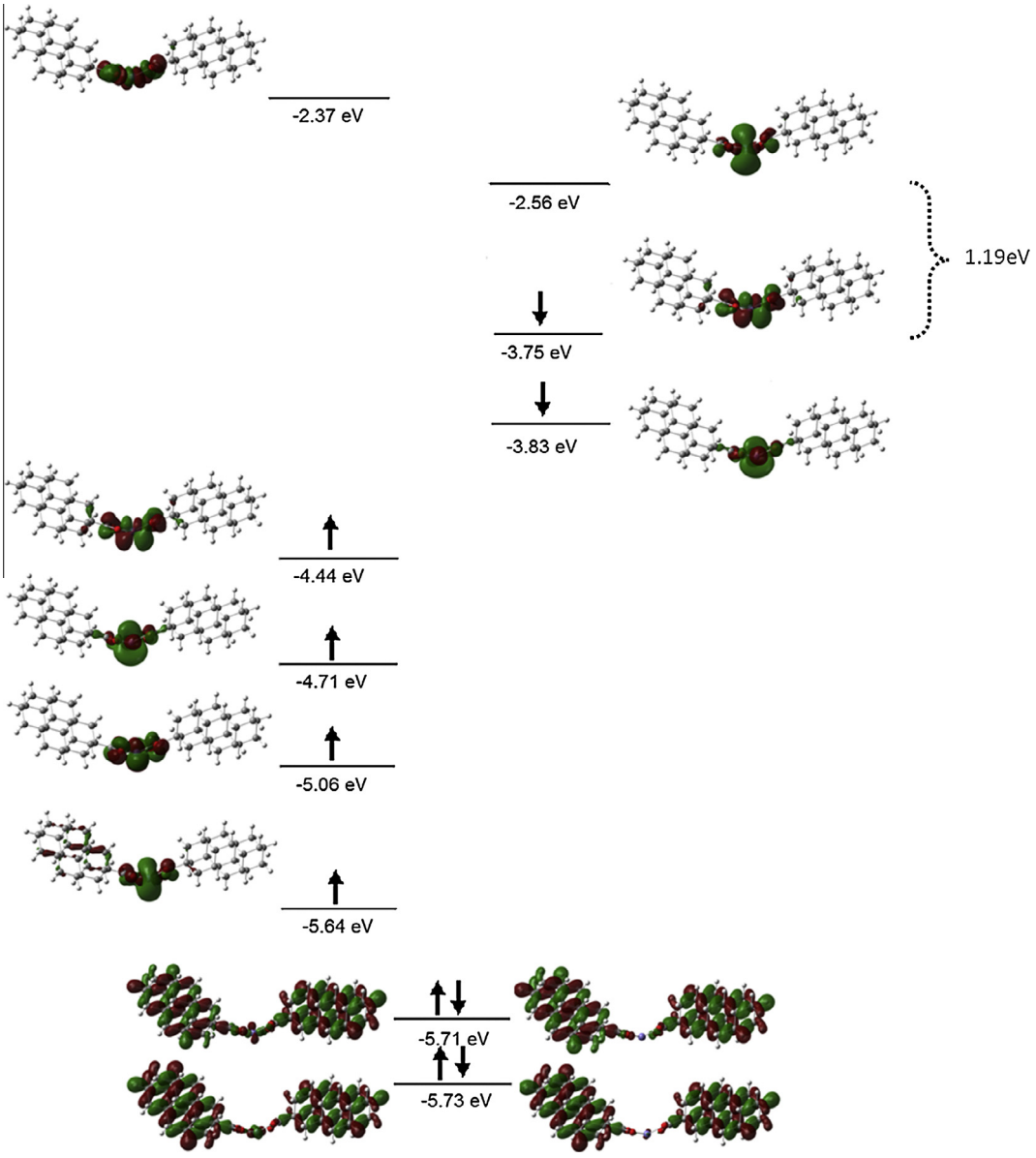

Fig. 6. Molecular orbital diagram and shape for the triplet of $C_{24}H_{27}O_4Fe$.

the LUMO? The answer is in the molecular orbital diagram presented in Fig. 5.

The LUMO manifests a trapping level very near the HOMO (~0.05 eV). Therefore, the resultant material is a conductor; practically a synthetic metal, but taking into account the difference when compared to LUMO+1, the corresponding shape and energy of these molecular orbitals is shown in Fig. 6. This configuration can be considered as an excited state, indeed the polarization of both electrons located on the HOMO taking advantage of the low energy empty molecular orbital easily leads to the description of a triplet. A new theoretical calculation was performed at the same level of theory but looking for the excited state, the result is very important because the triplet state is 26.48 kcal/mol lower in energy than the ground state. Therefore, this complex should have a defined magnetic moment and a paramagnetic behavior; in fact, the value of the magnetic moment is 2.1 μ_B, this is an indication that the triplet state should be a more stable item. The corresponding molecular orbital diagram is shown in Fig. 6.

Another interesting feature is that actually instead of two unpaired electrons there are six; however, this is not a septuplet because four of them have high spin whereas the other two have low spin. Therefore the global result is two unpaired electrons and the mentioned triplet state. This peculiar behavior deserves an explanation.

Fig. 7 shows a spin density map for ($C_{24}O_4Fe$), where the blue region corresponds to density for an unpaired electron in the occupied upper level. The green region corresponds to an electron density of unpaired electrons from level HOMO−1. Note that HOMO−1 level corresponds only to oxygen atoms, while the complete ligand region is involved in HOMO level.

The conductor and paramagnetic behavior could be only a legacy of the central complex, i.e. the iron atom and the carboxylic groups. Then the iron acetate complex was calculated in the same conditions in order to find the possible source of the anomalous behavior because if the characteristics were intrinsic of the acetate complex the substitution of nanodiamond would be obsolete. The calculation of the acetate complex yields a very different shape; this is an interesting substance because its energy gap corresponds to a weak conductor or semiconductor (0.94 eV). The corresponding molecular orbital diagram is shown in Fig. 8 and there are no trapping levels, the HOMO is a two folded degenerated set and the LUMO is a single molecular orbital separated almost 1 eV. The only similar feature is the shape of the center of the complex that has a slightly distorted symmetry D_{2d} (see Fig. 8) but all other results are different.

The anomalous behavior can be explained considering quantum-size effects found in nanodiamond in early works [15]. The nanodiamond unit $C_{22}H_{28}$ is an insulator and the quantum confinement makes it like an electronic reservoir box, however the introduction of the iron and the carboxylic groups gives place to a lack of electronic flow. Indeed, it can be considered that the energy levels of the coordination center go into the insulator

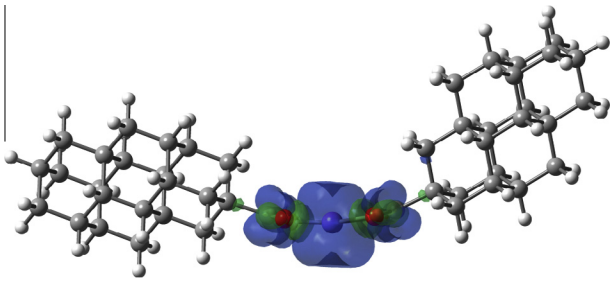

Fig. 7. Density spin map for ($C_{24}H_{27}O_4Fe$).

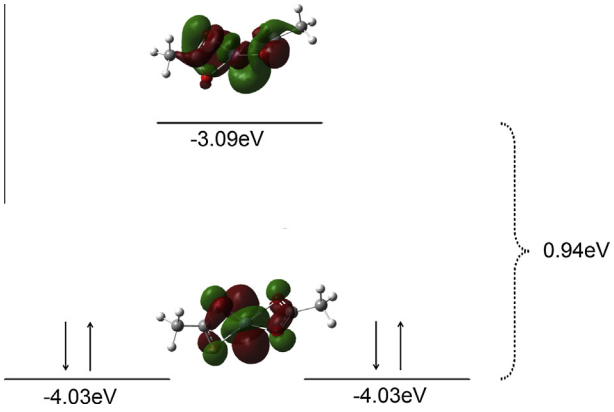

Fig. 8. Frontier molecular orbital diagram and shape of iron acetate.

"box" changing the situation to a conductor with paramagnetic properties, all the six unpaired electrons go to the iron and its ligands. Therefore the presence of nanodiamond is essential as well as the metal.

A last commentary should be made about the effect of the external carboxyl substituent on the nanodiamond ligands. As it was established above, the strong semiconductor behavior arises from the electronic confinement caused by the potential energy wall effect from the nanodiamond ligands. This effect is lost with the presence of the external ligands because the electrons have in this case a very important region for delocalization, very far from the center of the molecule (i.e. far from the iron atom). The global result is a behavior that resembles those of an insulator.

4. Conclusions

Coordination compounds of nanodiamond joint to an iron atom by means two carboxylic groups can have very different behavior than the pristine nanodiamond from a theoretical point of view. The case of an open compound with two nanodiamond units and carboxylic groups in the opposite ends is a normal semiconductor in strong contrast with the nanodiamond unit that is an insulator. The other case is that of a complex again with nanodiamond units but without the terminal carboxylic groups, this substance has conductor behavior but can stabilize an excited state with six unpaired electrons with different orientations, the global result is a triplet with strong paramagnetic behavior.

References

[1] (a) A.S. Barnard, S.P. Russo, I.K. Snook, First principles investigations of diamond ultrananocrystals, Int. J. Mod. Phys. B 17 (2003) 3865–3879;
(b) V.L. Kuznetsov, A.L. Chuvilin, Y.V. Butenko, I.Y. Malkov, V.M. Titov, Onion-like carbon from ultra-disperse diamond, Chem. Phys. Lett. 222 (1994) 343–348;
(c) M. Baidakova, A. Vul', New prospects and frontiers of nanodiamond clusters, J. Phys. D Appl. Phys. 40 (2007) 6300–6311;
(d) S. Mitura, Nanodiamonds, J. Achiev. Mater. Manuf. Eng. 24 (1) (2007) 166–171.
[2] A.I. Lyamkin, E.A. Petrov, A.P. Ershov, G.V. Sakovich, A.M. Staver, V.M. Titov, Production of nanodiamonds from explosives, Dokl. Akad. Nauk SSSR. 302 (1988) 611–613.
[3] A.L. Vereschagin, Detonation Nanodiamonds, Altai State Technical University, Barnaul, Russian Federation, 2001.
[4] J.P. Boudou, P.A. Curmi, F. Jelezko, J. Wrachtrup, P. Aubert, M. Sennour, G. Balasubramanian, R. Reuter, A. Thorel, E. Gaffet, High yield fabrication of fluorescent nanodiamonds, Nanotechnology 20 (23) (2009) 235602.
[5] (a) J.-Y. Raty, G. Galli, C. Bosteadt, T.W. Van Buuren, L.J. Terminello, Quantum confinement and fullerene like surface reconstructions in nanodiamonds, Phys. Rev. Lett. 90 (2003) 037401;
(b) A.S. Barnard, S.P. Russo, I.K. Snook, Ab initio modelling of band states in doped diamond, Philos. Mag. Lett. 83 (2003) 39–45.

[6] N.R. Greiner, D.S. Philips, J.D. Johnson, F. Volk, Diamonds in detonation soot, Nature 333 (1988) 440–442.
[7] V.V. Ivanovskaya, A.L. Ivanovskii, Atomic structure, electronic properties and thermal stability of diamond-like nanowires and nanotubes, Inorg. Mater. 43 (2007) 349–357.
[8] T. Patrusheva, V. Letunovsky, L. Goryacheva, A. Gorschkov, V. Sergienko, E. Jakovleva, Protective coatings from ultra fine diamond, Carbon 40 (2002) 125–135.
[9] (a) A.S. Barnard, M. Steruberg, Substitutional boron in nanodiamond, bucky-diamond, and nanocrystalline diamond grain boundaries, J. Phys. Chem. B 110 (2006) 19307–19314;
(b) A.S. Barnard, M. Steruberg, Substitutional nitrogen in nanodiamond and bucky-diamond particles, J. Phys. Chem. B 109 (2005) 17107–17112;
(c) V. Chu, J.P. Conde, J. Jarego, P. Brogueira, J. Rodríguez, N. Barradas, J.C. Soares, Transport and photoluminescence of hydrogenated amorphous silicon–carbon alloys, J. Appl. Phys. 78 (1995) 3164–3173.
[10] A.D. Becke, Density-functional exchange-energy approximation with correct asymptotic behavior, Phys. Rev. A 38 (1988) 3098–3100.
[11] J.P. Perdew, Y. Wang, Accurate and simple analytic representation of the electron-gas correlation energy, Phys. Rev. B 45 (1992) 13244–13249.
[12] M.J. Frisch, G.W. Trucks, H.B. Schlegel, G.E. Scuseria, M.A. Robb, J.R. Cheeseman, G. Scalmani, V. Barone, B. Mennucci, G.A. Petersson, H. Nakatsuji, M. Caricato, X. Li, H.P. Hratchian, A.F. Izmaylov, J. Bloino, G. Zheng, J.L. Sonnenberg, M. Hada, M. Ehara, K. Toyota, R. Fukuda, J. Hasegawa, M. Ishida, T. Nakajima, Y. Honda, O. Kitao, H. Nakai, T. Vreven, J.A. Montgomery Jr., J. E. Peralta, F. Ogliaro, M. Bearpark, J.J. Heyd, E. Brothers, K.N. Kudin, V.N. Staroverov, R. Kobayashi, J. Normand, K. Raghavachari, A. Rendell, J.C. Burant, S.S. Iyengar, J. Tomasi, M. Cossi, N. Rega, J.M. Millam, M. Klene, J.E. Knox, J.B. Cross, V. Bakken, C. Adamo, J. Jaramillo, R. Gomperts, R.E. Stratmann, O. Yazyev, A.J. Austin, R. Cammi, C. Pomelli, J.W. Ochterski, R.L. Martin, K. Morokuma, V.G. Zakrzewski, G.A. Voth, P. Salvador, J.J. Dannenberg, S. Dapprich, A.D. Daniels, Ö. Farkas, J.B. Foresman, J.V. Ortiz, J. Cioslowski, D.J. Fox, Gaussian 09, Revision A.1, Gaussian Inc., Wallingford, CT, 2009.
[13] K. Wolinski, J.F. Hilton, P. Pulay, Efficient implementation of the gauge-independent atomic orbital method for NMR chemical shift calculations, J. Am. Chem. Soc. 112 (1990) 8251–8260.
[14] D. Zhang, R.Q. Zhang, Signature of nanodiamond in Raman spectra: a density functional theoretical study, J. Phys. Chem. B 109 (2005) 9006–9013.
[15] A. Mizel, M.L. Cohen, Electronic energy levels in semiconductor nanocrystals: a Wannier function approach, Phys. Rev. Lett. 56 (1997) 6737–6741.